



Sensitivity of Ship Voyage Optimizations to Various Energy Cost Models

Downloaded from: <https://research.chalmers.se>, 2024-11-19 04:12 UTC

Citation for the original published paper (version of record):

Chen, Y., Mao, W. (2024). Sensitivity of Ship Voyage Optimizations to Various Energy Cost Models. International Conference on Offshore Mechanics and Arctic Engineering, Volume 5A: Ocean Engineering. <http://dx.doi.org/10.1115/OMAE2024-127986>

N.B. When citing this work, cite the original published paper.

SENSITIVITY OF SHIP VOYAGE OPTIMIZATIONS TO VARIOUS ENERGY COST MODELS

Yuhan Chen

Department of Mechanics and Maritime Sciences,
Chalmers University of Technology
Gothenburg, Sweden

Wengang Mao

Department of Mechanics and Maritime Sciences,
Chalmers University of Technology
Gothenburg, Sweden

ABSTRACT

A ship's energy performance model describing the relationship between ship speed and energy consumption is an essential component in her voyage optimization system, since it is required to evaluate the energy costs associated with different voyage plannings. For energy-efficient voyage planning, such a ship model estimates the corresponding energy consumption of each feasible route/sub-route based on her sailing speeds and encountering environmental conditions. Thus, the reliability of a ship's energy performance model is expected to have a great influence on the ship's voyage optimization results. Various approaches have been widely researched to construct the ship performance model, such as empirical white-box models based on experimental tests and physical knowledge, data-driven black-box models using machine learning methods, and gray-box models combining the above two approaches, etc. In addition, various energy cost functions are used for the ship voyage optimizations, such as the total power or fuel consumption, etc. The objective of this study is to investigate the sensitivity of ship voyage optimizations due to different energy cost functions from different modeling techniques. A chemical tanker with full-scale measurement is used in the case study to study the sensitivity of voyage optimizations in terms of energy efficiency. Some insights into employing different energy cost functions and models are discussed in detail to provide good recommendation practices for optimal voyage planning.

Keywords: Energy efficiency, machine learning, ship performance model, voyage optimization

1. INTRODUCTION

There is an increasing awareness in the shipping industry of the significance of reducing energy consumption. Besides saving costs for individual business companies, reducing energy consumption in shipping is crucial for combating climate change. Voyage optimization is a key factor in enhancing operational energy efficiency[23]. It involves comprehensive approaches that consider various factors such as weather conditions, vessel performance, and different optimization objectives, such as operation safety, efficiency, and accurate

estimated time of arrival (ETA). The ship performance model combines and evaluates these factors for specific objectives, offering evaluations for optimization cost functions, and supporting the decision-making. Thus, it is essential to integrate an accurate ship performance model that can provide robust assessments into voyage optimization for diverse sea conditions.

For energy-efficient ship voyage planning, optimization objectives can be defined in different ways, such as minimizing power[22], fuel[16], emissions[14, 23], or the overall economic/operational cost[2]. To evaluate the corresponding cost and identify the optimum solution, cost functions are essential to provide a quantitative measure of the performance or effectiveness of potential voyages. And based on the different objectives, the ship model is formulated and integrated into the cost function, to provide the relationship between the environmental conditions with factors that are of interest [25]. However, depending on the different optimization objectives, as well as diverse approaches to develop the ship performance model, the optimization process can vary and different impacts on the outcome can also be observed. Therefore, how these factors can influence the result, and their sensitivity to the optimization results is a topic worthy of exploration. In this paper, this topic is investigated focusing on how cost functions impact the optimization processes, and the sensitivity these factors exhibit to the optimization results.

For ship performance modeling, many approaches have been developed and explored. They can generally be divided into empirical or semi-empirical formulations, computational fluid dynamics (CFD) methods, model testing, and machine learning (ML) approaches[6, 7, 10, 19]. Among which, empirical/semi-empirical techniques are widely used in today's voyage optimization, which are based on fundamental laws of physics and prior knowledge that can ensure reliable predictions under various conditions. They are cost-effective to develop and have good extrapolability beyond the given data. Also, machine learning (ML) techniques and Artificial Intelligence (AI) come with great possibilities to develop accurate ship performance models, allow for reliable energy efficient measures, and reduce greenhouse gas (GHG) emissions. Various research and commercial developments have produced promising results[1, 8, 15, 18, 24]. A substantial amount of ship operational data can be

gathered through onboard sensors for real-time monitoring[4], and ML models can be built upon these measurement data.

However, the empirical methods can be complicated and may generalize complex phenomena with assumptions, which may not account for unique or unexpected sea conditions and operations. These uncertainties related to traditional physical models have been found and acknowledged by the maritime industry[4, 20]. And machine learning methods rely on the quantity and quality of the full-scale measurement data, and may result in unreasonable results for unseen scenarios with less satisfying extrapolation capabilities. When integrated into the voyage optimization system, there can be uncertainties if these characteristics of ship models have different impacts on voyage optimization functionality, and lead to different deviated optimal outcomes. Further, since the cost function that involves the ship model is essential for the optimization process, the sensitivities of the different ship models on the voyage optimization should also be investigated.

In this paper, the impact of the ship performance model on energy-efficient voyage optimization is investigated, by estimating different energy costs in terms of power and fuel, also using AI/ML techniques and theoretically/empirically developed models respectively in voyage optimization considering accurate ETAs. The introduction to voyage optimization and the optimization algorithm used in this study are presented in Section 2. Following that, the ship models are integrated into cost functions, and these five cost functions based on different strategies are presented in Section 3. The ship models' influence on voyage planning is validated with a case study ship, and the optimization results by employing different ship models will be compared in Section 4, followed by conclusions in Section 5.

2. VOYAGE OPTIMIZATION FOR SHIP OPERATION

2.1. Overview of energy-efficient voyage optimization

A general scheme of energy-efficient voyage optimization systems for seagoing vessels is presented in Figure 1. A typical voyage optimization system requires three major components, the weather/metocean conditions, the ship performance model within the cost evaluations, and a voyage optimization algorithm to effectively execute the voyage optimization process complying with specific optimization objectives.

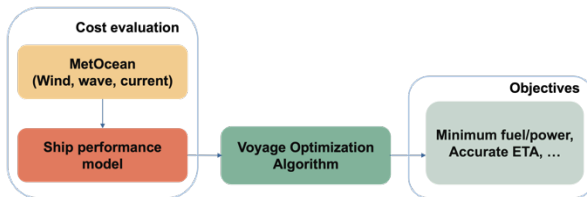


FIGURE 1: GENERAL SCHEME OF VOYAGE OPTIMIZATION

For a given voyage, the sailing area between departure P_0 and destination P_f will be initially discretized into time stages and partitioned into a waypoint grid. Each waypoint inside the grid is defined as:

$$P_{i,j} = [x_{i,j}, y_{i,j}, t_{i,j}] \quad (1)$$

The subscript i represents the number of the current time stage, and j represents the number of waypoints at the current time stage. The edges between the feasible waypoints represent the sub-routes, and within each sub-route, the sailing speed can be determined based on the required arrival time, or used as a control variable to be optimized by the algorithms. This grid can be generated either statically or dynamically, based on different strategies from various optimization algorithms.

Weather conditions have a great impact on the overall energy cost. Therefore, its voyage optimization often incorporates weather-routing problems by considering how weather conditions affect fuel consumption. The weather/metocean condition $W(P)$ based on the waypoint variable P can be presented as follows:

$$W(P) = [S(\omega|H_s, T_z), V_c, \theta_c, V_w, \theta_w] \quad (2)$$

where $S(\omega|H_s, T_z)$ represents the encountered waves in terms of significant wave height H_s and wave period T_z . V_c , θ_c , V_w , and θ_w include the ocean current and wind conditions respectively, i.e., the speed V and moving directions θ .

Then, this weather influence is evaluated by the ship performance model as the energy cost of waypoint $P_{i,j}$. That is, the ship model in the cost function will estimate the corresponding energy cost to reach $P_{i,j}$ through the preceding sub-route, provided with the waypoint state (e.g., speed), and weather forecast with metocean data $W(P)$. The cost function C_p can be then presented as:

$$C_p = f(W(P)) \quad (3)$$

The optimization aims to find the route with the lowest accumulative cost of all sub-routes. Thus, based on the cost given by the cost function in Eq. (3), the voyage optimization system could perform the decision-making to identify the most energy-efficient route that meets the optimization objective.

Finally, the optimal route R^* is obtained with waypoints in a series:

$$R^* = [P_0, P_{1,j_1}, \dots, P_{i^*,j^*}, \dots, P_f] \quad (4)$$

However, the sailing area normally contains a substantial number of waypoints. For each potential sub-route/waypoint, its associated cost is evaluated following environmental conditions, depending on individual positions and passing time. This may contain unseen situations beyond measurement, thereby requiring a robust data processing capability to provide reliable and accurate prediction for diverse conditions. Then it will be able to provide a solid foundation for the decision-making process of the optimization algorithm; otherwise, the optimization results will be grounded on inaccurately perceived information, which could lead to ineffective planning for the actual voyage. In this study, five empirical and ML ship models

are presented in the following Section 3, which are based on different development methods to provide the relationship between sailing speed to corresponding energy consumption for the voyage optimization algorithm.

2.2. 3D Dijkstra voyage optimization algorithm

The voyage optimization algorithm used in this study is the three-dimensional Dijkstra algorithm (3DDA)[21]. The Dijkstra algorithm[5] is a widely recognized computational algorithm used in graph theory for solving the shortest path problem. It has become a common approach in the field of computer science particularly in network routing and navigation, and stands out for its efficiency and accuracy in determining the shortest route between a starting point and the destination in a weighted graph, with edges representing sub-routes with costs like distance or time.

For energy-efficient sailing, the Dijkstra algorithm is utilized to determine the most efficient route for a ship, such as in 3DDA. The 3DDA method is a recent and advanced implementation of the Dijkstra algorithm specifically extended and refined for use in open sea navigation. It involves finding the lowest-cost route in coordinates (longitude and latitude), along with an optimized speed profile in a waypoint grid that represents various potential maritime trajectories.

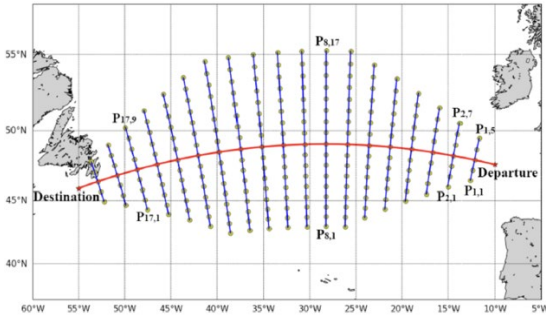


FIGURE 2: SPATIAL WAYPOINT GRID OF 3DDA TO DISCRETIZE THE SAILING AREA[21].

For a given voyage, to perform the 3DDA method, first, a reference route in the middle, shown as the red line in Figure 2, needs to be chosen either the great circle route or based on experience. Then the sailing area between the departure and destination is initialized with discretized time stages, with a waypoint grid in the spatial region. Each waypoint is defined as $P_{i,j}$ in Eq. (1).

The control variable $U(P)$ for optimization includes:

$$U(P) = [v, \theta] \quad (5)$$

where v is the interval sailing speed in the following sub-route after P , and θ indicates the course angle of the ship. Therefore, the 3DDA method effectively carries out voyage optimization by considering both position and speed variations.

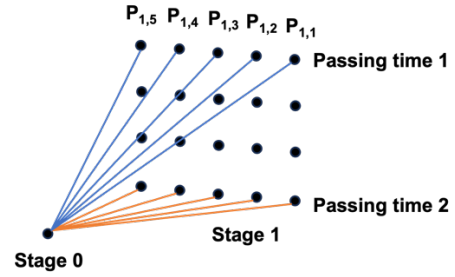


FIGURE 3: THE 3D GRAPH FOR STAGE 1 WAYPOINTS OF 3DDA METHOD

The waypoints at adjacent time stages in the spatial grid are free to explore their way to the next stage's waypoints, and they will relate to the adjacent predecessors and their successors by directed edges, indicating the sub-routes. Meanwhile, to take into account the speed variation, which in this study is chosen as in the range $[0.5v, 1.2v]$, each waypoint also possesses different passing times. Thus, the grid is also expanded to an additional time frame. The 3D graph for waypoints in Stage 1, i.e., $P_{1,1}$ to $P_{1,5}$, in Figure 2, is shown in Figure 3 with connected edges representing voyage legs. The passing time varies in a range which is determined with a fixed time difference Δt , and Δt is chosen as 15 minutes in this study. The overall associated speeds should be within $[0.5v, 1.2v]$. The upcoming spatial stages, i.e., $P_{2,j}$, and the following stages are all expended in this way in the time dimension, and the entire 3D graph for the search space can then be obtained.

Each edge/sub-route in this three-dimensional graph is weighted with an energy cost as in Eq. (3). The cost function in 3DDA is defined as:

$$C_p = f(U(P), W(P)) \quad (6)$$

The formulation of the cost function is directly related to the ship performance model, to determine the corresponding engine power cost or fuel cost using either empirical or ML techniques, based on the optimization control variable $U(P)$ and environment states $W(P)$ for each sub-route. The different ship models employed and compared in this study will be further presented in Section 3. Finally, the grid will be searched by the Dijkstra algorithm for the optimal route with the lowest accumulative energy cost C_p , composed of discretized sub-routes as Eq. (4), along with a corresponding optimal control set of $U(P_{i,j})$.

The strength of the 3DDA algorithm lies in its ability to consider the joint optimization of route and speed by processing a vast network of waypoints and routes. Provided that its grid resolution is sufficient, it can find the optimal route in the grid with robustness while also ensuring arrival punctuality for real operations.

2.3. Encountered metocean conditions

For voyage optimizations, the uncertainties that influence the result can generally appear in the weather, cost function (ship model), and algorithm optimization capabilities. In this case

study, the hindcast weather data are used to avoid the uncertainties from the weather, as all encountered MetOcean environmental data inputs (wind, wave, and current) that the ship performance model demands to estimate power/fuel. Related MetOcean parameters are extracted from ECMWF ERA-5 (2023) dataset for wind and wave, and ocean current data is acquired from Copernicus 2023 server. An example of encountered waves represented by significant wave height is shown in Figure 4.

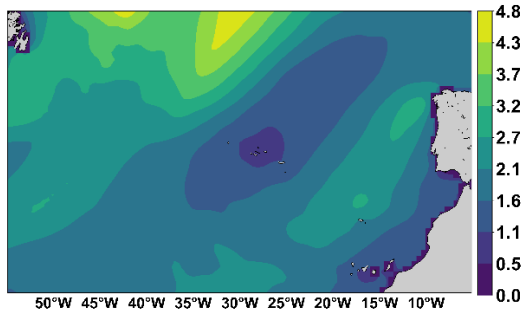


FIGURE 4: CONTOUR PLOT FOR SIGNIFICANT WAVE HEIGHTS IN NOVEMBER 2016 FROM ECMWF DATASET

3. COST FUNCTIONS WITH DIFFERENT SHIP PERFORMANCE MODELS

As outlined in the above voyage optimization procedures, the control variables $U(P)$ include the ship's sailing speed, thus the performance model in this study is supposed to predict the energy cost for the required v . To develop the ship performance model and acquire performance-related factors such as power and fuel consumption, the general procedure typically adheres to the following sequence, as in Figure 5. First, the hull resistance is associated with the ship's cruising speed, i.e., speed through water, and the encountered sea states. The propulsion power can then be computed based on the propeller's effective power against the resistance, engine configurations, and propeller efficiencies. And finally, the fuel consumption is obtained through Specific Fuel Oil Consumption (SFOC), representing the efficiency of the ship engine.

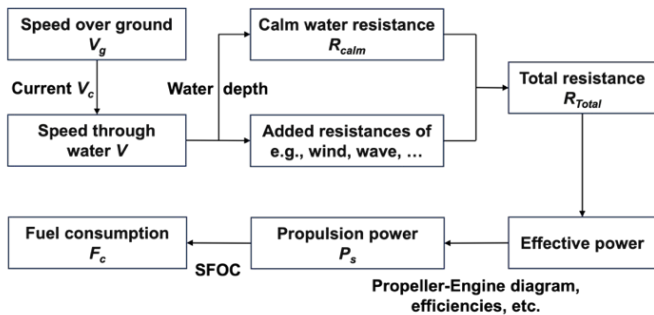


FIGURE 5: SHIP ENERGY CONSUMPTION ESTIMATION PROCESS

To achieve energy-efficient sailing with accurate arrival time, the objective of voyage optimization is set as the minimum

energy consumption along a voyage, and the ETA of voyage planning is set the same as the selected case study voyages. The differences among different approaches are primarily reflected in the construction of cost functions in voyage optimization, where the ship performance model is employed. To achieve the objective of minimum energy usage, the cost function can either be chosen as the minimum engine shaft power, or the minimum total fuel consumption. The relationship between engine power P_s and fuel consumption F_c is as follows:

$$F_c = P_s \times SFOC \quad (7)$$

The power P_s could be acquired from the ship performance model providing the ship's speed-power relationship. SFOC is the engine efficiency that can vary under different sailing speeds. In the industry, the SFOC curve is calibrated through a series of testing and data analyses using Eq. (7). Thus, both the speed-power relationship and the SFOC coefficient can either be obtained using statistical regression based on empirical knowledge or using AI/ML models with measurement data. Similarly, the empirical SFOC curve can provide the mean value of SFOC within the measured time interval. However, there still contains large uncertainties/discrepancies of SFOC between measured and its theoretical value provided by manufactures, as shown in Figure 6. Its accuracy can still be increased to involve comprehensive factors under diverse operation conditions.

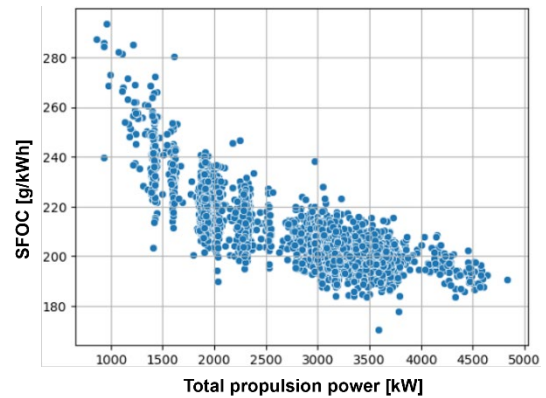


FIGURE 6: MEASURED SFOC VALUE UNDER DIFFERENT OPERATION CONDITIONS

In the voyage optimization, the objective can be chosen to either minimize the total resistance of ship R_{Total} , engine power P_s , or the final fuel consumption F_c to achieve the energy efficiency. However, from Figure 5, it can be seen that due to the hull-propulsion-engine coupling, the efficiencies of the engine and propeller are also significant for the final energy cost. And if only to consider the single resistance or power, the result can be different from considering fuel in the optimization. Similarly, SFOC may also change under actual operational conditions, which may further lead to discrepancies in fuel calculation and deviate voyage optimization. The impact of all these factors can be identified, however, how these factors can influence the voyage optimization needs to be further investigated.

It is worth noting that, the concept of SFOC is not only limited to fuel oil, instead, it is a universal metric that can also be applied to alternative fuels such as LNG (Liquefied Natural Gas), methanol, and ammonia. The principle behind SFOC remains the same for these fuels, which reflects the engine's capability to transfer the fuel's energy into useful work. Given the varying energy densities and combustion properties of LNG, methanol, and ammonia compared to conventional fuels, engines using these fuels may possess different SFOC values/curves. However, the similar estimation process is still applicable.

Therefore, in this paper, five cost functions are first constructed to reflect the different optimization objectives, based on different ship performance models as illustrated in Table 1. Further, the cost functions are integrated respectively in the 3DDA voyage optimization method, and their impacts on the optimization result are compared in Section 4.

Table 1: DIFFERENT PERFORMANCE MODELS USED FOR THE COST FUNCTION

Model	Speed-Power	SFOC
Speed-power empirical	Empirical	-
Speed-fuel empirical	Empirical	Empirical
Speed-power ML	ML	-
Speed-fuel ML	ML	Empirical
ML SFOC	ML	ML

3.1. Speed-power empirical model

One feasible option to optimize the overall voyage sailing cost is to achieve the minimum shaft power, since it is directly related to the total work done by the engine. The power consumption model is also the easily accessible performance model that shipping companies can get from towing tank tests during their design stage. The cost function could estimate the shaft power based on the given speed. In this part, the presented ship performance model is developed based on an empirical approach. The workflow of such a speed-to-power model is shown in Figure 5.

The first parameter that should be initially determined is the ship's speed through water V . According to the approximation in ISO15016[17], the speed through water V can be obtained by the speed over ground V_g and ocean current speed V_c using the superposition principle:

$$V = V_g + V_c \quad (8)$$

Then, based on the encountered sea states and the ship's characteristics, the total resistance of the ship R_{Total} is derived by summing calm water resistance R_{Calm} , and added resistances of wind R_{Wind} , wave R_{Wave} , current R_C , and shallow water R_S , i.e.,

$$R_{Total} = R_{Calm} + R_{Wind} + R_{Wave} + R_C + R_S \quad (9)$$

The thrust forces from the engine and propellers counteract this total resistance R_{Total} to push the ship forward. Therefore, the overall shaft power P_S that the engine needs to produce can be obtained based on the total resistance R_{Total} , using the engine's work efficiency and configurations provided by manufacturers. This is a conventional way of ship performance estimation. Here, the calm water resistance and all the added resistance to influence the ship's motion are computed respectively, based on the work proposed in [11, 12]. And finally, the shaft power P_S can be derived as follows:

$$P_S = R_{Total} \times V / \eta \quad (10)$$

where η is the efficiency coefficient including the hull efficiency, propeller open water efficiency, and engine shaft efficiency, calculated based on[9]. For such an empirical method, it does not include the uncertainties during sailing in the speed-power estimation such as statistical waves and various coefficient changes due to fouling, etc. It is hard to present a highly precise speed-power relationship using semi-empirical and theoretical models, however, it could provide acceptable accuracy both in interpolation and extrapolation that include situations beyond measurement. Besides, since the computational speed is significant for the performance of a voyage optimization algorithm, an empirical model would bring fewer computation loads, compared with other comprehensive methods that are highly accurate, such as advanced machine learning models.

3.2. Speed-fuel empirical model

More practically, the cost function can also be directly formulated to optimize the overall fuel cost to achieve energy efficiency. Based on Section 3.1, to further determine the fuel consumption concerning a given shaft power, Specific Fuel Oil Consumption (SFOC) coefficient should be calculated as outlined in Eq. (7). SFOC is a critical metric in the maritime industry, used to represent the efficiency of a marine engine. It represents the amount of fuel consumed by the engine relative to its power output over a certain period. Essentially, it measures how much fuel is needed to produce a specific amount of power, therefore it is a key indicator of marine engine efficiency. Lower SFOC indicates a more fuel-efficient engine that generates more power with less fuel, leading to reduced operating costs and lower emissions. Conversely, higher SFOC values indicate less efficient fuel usage, which translates to higher costs and increased emissions.

In this part, the cost function is further formulated to provide the fuel cost based on the engine power P_S . The theoretical curve of SFOC is regressed as a cubic polynomial using measurement data of F_c and P_S , and the relationship between the specific SFOC based on P_S is described as shown in Figure 7. Combined with the empirical speed-to-power ship model introduced in Section 3.1, first to get P_S , and input it in the regressed $P_S - SFOC$ cubic curve to get the corresponding SFOC value, the fuel cost F_c can be obtained as presented in Eq. (7).

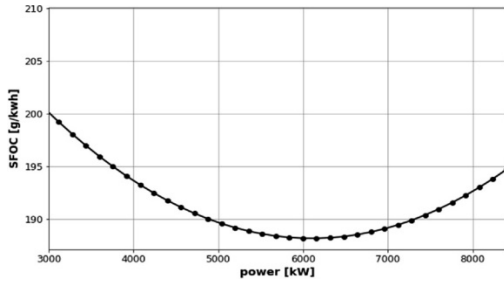


FIGURE 7: REGRESSED EMPIRICAL SFOC CURVE USED IN THIS STUDY FOR THE CASE STUDY SHIP

3.3. Speed-power machine learning model

Current studies and industry advancements have yielded promising outcomes in the development of ML models capable of predicting ship performance under diverse conditions and offering suggestions for more efficient ship operations. Various machine learning methods can be implemented in describing the speed-power relationship of ships, and different models have been developed and compared to investigate the most suitable method for ship performance modeling with the least discrepancies[13]. It can be found that XGBoost method could provide no more than 3% accumulative discrepancy in power prediction for more than 10 days of actual sailing, while the other methods, i.e., neural network, support vector regression, generalized additive model, and statistic methods (linear and polynomial regression) show around 20%-30% discrepancy.

XGBoost (Extreme Gradient Boosting) is an advanced and efficient implementation of gradient boosting, a machine learning technique used for regression and classification problems[3]. It has gained popularity due to both its performance and speed in data modeling and processing. Therefore, the XGBoost method is employed in this section as the ML technique to develop the speed-power model, and the cost function utilizes the XGBoost model to obtain the evaluation of engine shaft power as an ML approach, in comparison with the empirical approach introduced in Section 3.1.

For the ship's shaft power prediction, the prediction output y is the measured shaft power P_s , and the input features consist of all the elements included in variables $U(P)$ and $W(P)$, in addition to the ship draft. The dataset is then given into the XGBoost method for model development and evaluation. Finally, the trained XGBoost model is integrated into the 3DDA algorithm to achieve optimized engine power for the voyage optimization.

3.4. Speed-fuel machine learning model

In this part, the cost function is formulated to estimate the fuel cost, and the XGBoost speed-power model introduced in Section 3.3 is employed to replace the empirical power evaluation. The value of the SFOC coefficient is further needed, and here it is obtained through the $P_s - \text{SFOC}$ cubic regression empirical method, same as in Section 3.2. This is for the comparison with the machine learning SFOC model that will be presented in the following section.

3.5. SFOC machine learning model

Several factors can influence an engine's actual SFOC, including its type and design, operating conditions, and maintenance practices. For a specific marine diesel engine, its SFOC is significantly affected by the engine operation/setting parameters and its interactions with ship resistance/propulsion systems. Moreover, the actual operating conditions often differ from the ideal or test conditions under which the theoretical SFOC is determined which leads to deviations from the reference values. Factors such as load variations, sea state, hull condition (such as fouling, mechanical wear, and maintenance), and ambient temperature can all influence the actual engine performance, especially as operational time proceeds.

For the performance model, SFOC is one of the significant elements that the estimation of fuel consumption depends on. If the value of SFOC fails to reflect the actual operation's real value, the voyage optimization's decision can also lead to great deviations. It not only causes sub-optimal voyage optimization such as consuming more fuel than expected, but also can make the ship not capable of following the scheduled ETA, since the planned power/fuel is based on an inaccurate estimation. Moreover, when ships are sailing in a dynamic marine environment, the variation of ship resistance and propulsion efficiency can lead to continuous adjustment of marine engine settings to keep ships' pre-defined navigation patterns. The combination of dynamic sailing marine environments and engine setting variations may cause actual engine SFOC to differ significantly from the provided SFOC curve. These differences could further lead to deviations in sailings, which may continuously accumulate as the voyage proceeds.

In this part, a data driven SFOC model is established by machine learning techniques. The impact of more accurate SFOC machine learning models in comparison with empirical SFOC curves given in Section 3.2, is briefly studied by demonstrating their application to evaluate a ship's energy performance along her actual voyages.

4. COMPARISON OF SHIP MODELS' IMPACT ON VOYAGE OPTIMIZATION

In this study, the sensitivity of the optimization result to different cost functions including ship models, is investigated using a case study ship along with her actual voyages. The case study ship is presented in Section 4.1, and the optimization results, due the characteristics of voyages in different directions, are compared in terms of westbound and eastbound voyages in Section 4.2 and Section 4.3 respectively.

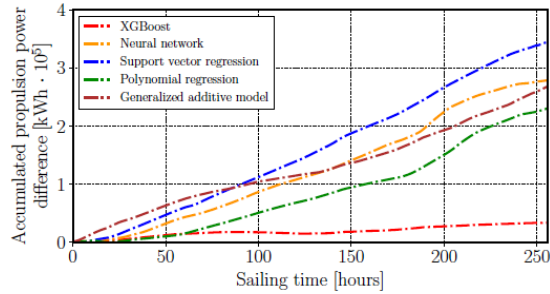
4.1. Case study ship

A chemical tanker with full-scale measurement is used in this case study, with main particulars given in Table 2. A conventional weather routing system was installed on the ship to guide the voyage planning. Combined with the ship master's experience, the actual sailing routes are supposed to be more efficient than ordinary voyage planning systems. Four voyages

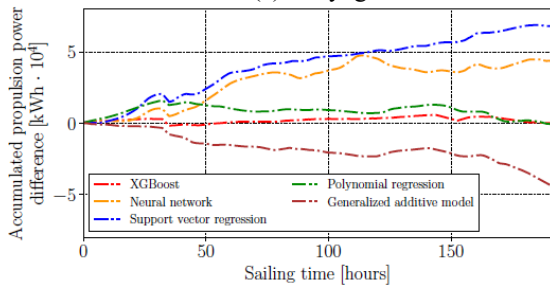
of the actual ship measured at North Atlantic in 2015 and 2016, including westbound and eastbound, during winter and summer, are selected as the case study voyages for result comparison.

Table 2: PRINCIPAL PARTICULARS OF THE CHEMICAL TANKER SHIP

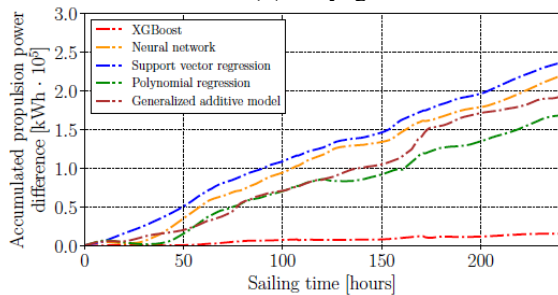
Length L_{oa}	178.4 m	Design draught	10.98 m
Length L_{pp}	174.8 m	Block coefficient	0.8005
Beam B	32.2 m	Deadweight	50752 t
Depth	17.0 m		



(a) Voyage 1



(b) Voyage 2



(c) Voyage 3

FIGURE 8: THE ACCUMULATED PROPULSION POWER DIFFERENCE BY THE DIFFERENT MACHINE LEARNING ALGORITHMS IN[13].

Ship performance models built by different methods as listed in Table 1 are employed in the cost function, and ML models developed by XGBoost method are chosen and developed for the result comparison with the traditional empirical models. As shown in Figure 8, it can be seen that the ML method XGBoost can present considerably low prediction accumulative errors in more than 150-hour voyage sailings for three typical voyages. Besides, it also shows the best performance prediction compared to other ML methods. Thus,

the XGBoost model is chosen as the ML model in this case study. Based on these models, five different cost functions are constructed for the voyage optimization algorithm, to minimize the shaft power from the engine, and the fuel consumption respectively.

In addition, the cost functions are integrated into the recently developed algorithm 3DDA method. To deploy the 3DDA, its grid has a great impact on the optimization result and needs to be configured for initialization. For the four voyages, the grid of 3DDA is specified based on the actual ETA and sailing ranges. And for each of the voyages, the grid is kept the same to compare only the effect of changing the cost functions. Meanwhile, the actual fuel consumptions of these case study voyages are also estimated using the ML ship model based on actual data, to provide more accurate fuel estimation and exclude measurement errors.

4.2. Westbound voyage optimization

Two westbound voyage cases are used in this part for optimization validation, with optimized routes presented in Figure 9 and Figure 10. The weather changes in both two cases are not dramatic, and the highest significant wave heights is no more than 4 meters as shown in Figure 11 and Figure 12. These two cases present the normal and calm sailing status for ships operating in the North Atlantic Sea. The optimization results by changing different cost functions are listed in Table 3, where the fuel consumption is given both in amount and the reduction percentage compared to the actual fuel cost. The actual fuel consumption is estimated by the ML ship model to provide the most accurate estimation of the actual cost.

Table 3: OPTIMIZATION COMPARISON FOR EMPLOYING DIFFERENT SHIP PERFORMANCE MODELS

Models	Fuel consumption[ton]			
	Voy. 20161108		Voy. 20150721	
	Amount	%	Amount	%
Actual ship	177.9	-	178.5	-
Speed-power empirical	163.1	8.4	178.0	0.3
Speed-fuel empirical	162.3	8.8	165.9	7.0
Speed-power ML	154.6	13.1	151.4	15.2
Speed-fuel ML	154.3	13.3	151.3	15.2
ML SFOC	161.3	9.3	161.3	9.6

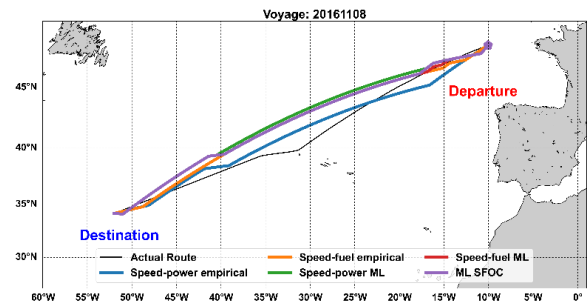


FIGURE 9: OPTIMIZED ROUTES BY DIFFERENT COST FUNCTIONS FOR CASE VOYAGE 20161108

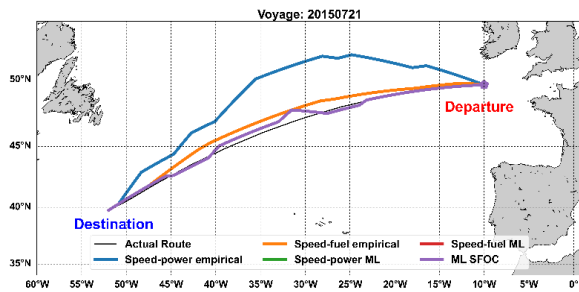


FIGURE 10: OPTIMIZED ROUTES BY DIFFERENT COST FUNCTIONS FOR CASE VOYAGE 20150721

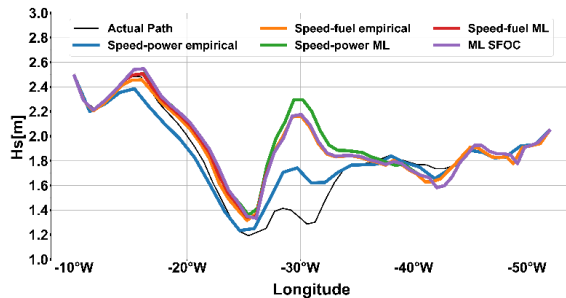


FIGURE 11: SIGNIFICANT WAVE HEIGHT ENCOUNTERED ALONG VOYAGE 20161108

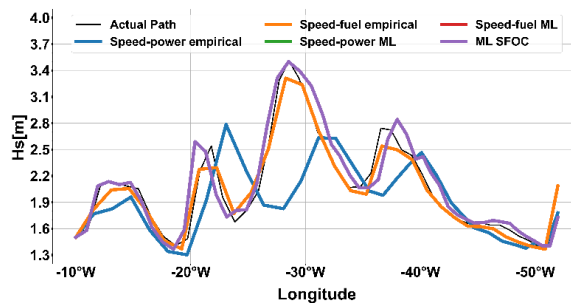


FIGURE 12: SIGNIFICANT WAVE HEIGHT ENCOUNTERED ALONG VOYAGE 20150721

From Figure 9 and Figure 10, it can be seen that the actual routes for both cases have undergone a well-considered planning process. The routes in general do not deviate much from the shortest Great Circle route, leading to a relatively short total distance, and their encountered weather conditions are also calm. Especially for the case Voyage 20161108, the actual route adjusts its heading twice to keep sailing in very calm waves. Therefore, the actual fuel consumption for both cases is not very high. For such calm sailing cases, a fuel reduction of around 5% from voyage planning compared with the actual route can be considered significant. However, from the result shown in Table 3, the result of total fuel consumption fluctuates greatly in the amount due to the change of the ship model and the cost functions.

Firstly, for fuel savings, the three cost functions by ML techniques, i.e., ML speed-power and speed-fuel model, including the ML SFOC model, all present a higher reduction for both two cases. Specifically, in the summer Voyage 20150721 where the sea status becomes more varying, the divergences in

the fuel consumption become more noticeable compared with the other very calm sailing case Voyage 20161108. Moreover, to compare the difference in optimizing the power and fuel cost, in this summer Voyage 20150721, the empirical models also present more apparent deviations both from the route and fuel cost. The empirical model in speed-power leads to 0.3% fuel savings, while the empirical model of speed-fuel shows a result of 7.0%. The two ML ship models result closely in both cases, contributing up to around 13% and 15% respectively. However, when considering the effect of SFOC, the result both changes to around 9%.

For the suggested routes shown in Figure 9 and Figure 10, it can be seen that the routes given by the two empirical models, i.e., optimizing power and fuel, are diverged and mostly do not overlap. Moreover, in Figure 10, the route from the speed-power empirical model suggests a noticeable long detour, which explains its relatively high fuel cost with only 0.3% savings, while choosing fuel as energy cost can lead to 7.0%. It may be due to using the power cost as the optimization objective can neglect the effect of long-distance and only opt for the lower power, thereby leading to local optimizations. This corresponds to the encountered H_s during the voyage shown in Figure 12, where the speed-power empirical function leads to the lowest waves in general compared to others. And similar situation can also be observed in the other case Voyage 20161108. Optimization results using ML models present closer results in both two cases, with similar suggested routes, fuel savings, and encountered sea states. In Figure 10, three routes by ML models are completely overlapped. However, due to the estimation by different ship models, i.e., considering the changes of actual SFOC value, the estimation of fuel consumption from ML SFOC is updated, therefore leading to different amounts of fuel consumption and savings.

4.3. Eastbound voyage optimization

Two eastbound voyage cases are included in this section. Due to the natural environment in the North Atlantic, eastbound voyages can bring a higher possibility for ships to come across storms. Among these two cases, one winter voyage experienced extremely severe weather changes and encountered very harsh sea conditions, where the highest H_s reaches more than 9 meters as shown in Figure 15. And the other summer voyage is a rather normal sailing case that H_s has reached more than 5 meters as in Figure 16. Their actual routes, which are shown in Figure 13 and Figure 14 can also reflect the situations. The route of the winter Voyage 20160229 diverges far away from the Great Circle route to adapt to the weather situations. And the route of the summer Voyage 20160523 generally follows the Great Circle route, mainly opting for the shortest distance sailing.

For the harsh sea sailings in winter, fuel consumption can result in dramatic changes if the voyage planning is inefficient. For a normal voyage, it is also considerable if more than 5% of fuel usage can be saved. However, the optimization result listed in Table 4 can still present considerable differences in fuel savings.

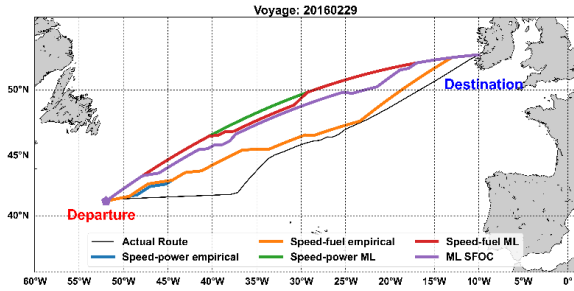


FIGURE 13: OPTIMIZED ROUTES BY DIFFERENT COST FUNCTIONS FOR CASE VOYAGE 20160229

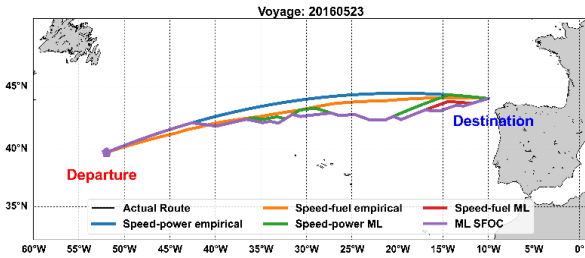


FIGURE 14: OPTIMIZED ROUTES BY DIFFERENT COST FUNCTIONS FOR CASE VOYAGE 20160523

Table 4: OPTIMIZATION COMPARISON FOR EMPLOYING DIFFERENT SHIP PERFORMANCE MODELS

Models	Fuel consumption[ton]			
	Voy. 20160229		Voy. 20160523	
	Amount	%	Amount	%
Actual ship	174.8	-	174.2	-
Speed-power empirical	152.0	13.0	152.0	12.7
Speed-fuel empirical	151.8	13.2	150.9	13.4
Speed-power ML	145.3	16.9	149.4	14.2
Speed-fuel ML	143.7	17.8	149.2	14.4
ML SFOC	150.6	13.8	158.8	8.8

In these two eastbound voyages, to compare the difference in optimizing the power and fuel cost, the results of fuel savings from the two empirical models are rather close, with both around 13%. However, the differences in routes and encountered weather can still be observed. Moreover, the empirical cost functions still do not contribute as much as ML cost functions do in improving energy efficiency, which is similar to the westbound cases in the above sections. Using the ML speed-power and speed-fuel models provides around 17% and 14% fuel reduction respectively for two cases. Although they still stably present fuel savings close to each other in these two diverse environments sailing cases, their suggested routes and encountered environmental conditions are also different, especially in the case Voyage 20160229. Meanwhile, it is worth noticing that obvious differences are also presented in this case when including the SFOC calculation using ML techniques. The fuel reduction from the ML SFOC model increases to 13.8%, and an entirely different route is also suggested as presented in Figure 13. Since this case involves more dramatic changes in environmental conditions, this change may also cause more

apparent changes in SFOC value, further leading to more different optimization results. On the contrary, in the other case Voyage 20160523, the result of ML SFOC does not show obvious deviations, and its encountered sea conditions generally overlap with the ML speed-fuel model. However, these two eastbound voyages both involve greater changes in the environmental conditions compared with the above westbound cases, and more apparent deviations can also be noticed between using the power and fuel cost as the optimization objectives.

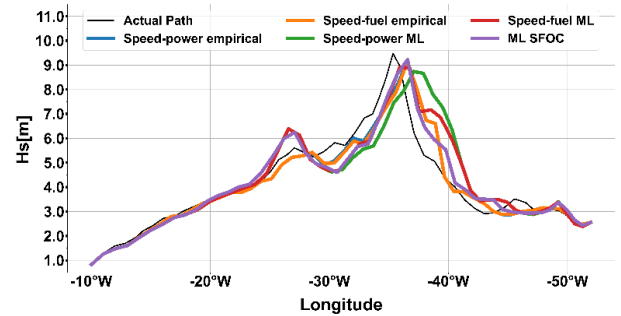


FIGURE 15: SIGNIFICANT WAVE HEIGHT ENCOUNTERED ALONG VOYAGE 20160229

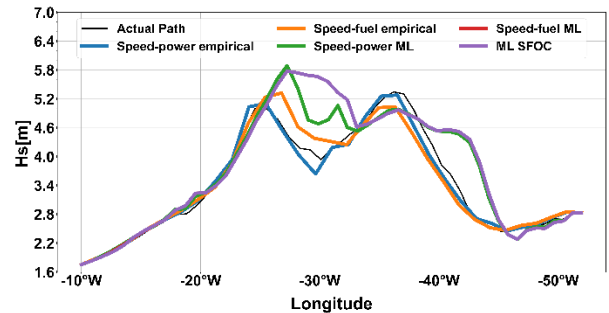


FIGURE 16: SIGNIFICANT WAVE HEIGHT ENCOUNTERED ALONG VOYAGE 20160523

5. CONCLUSION

Voyage optimization is an essential means of achieving energy-efficient navigation, which is sensitive to the energy cost function to support its decision-making. In this study, five cost functions are formulated to investigate the impact of different energy costs as the optimization objectives on voyage optimization results, integrating ship models in different approaches. The employed ship models are developed in empirical and machine learning approaches, and the cost functions are constructed to evaluate the energy cost in terms of power and fuel respectively, while also considering the variations of the engine efficiency SFOC under different operational conditions. A state-of-the-art and well-developed three-dimensional Dijkstra (3DDA) method is used as the optimization algorithm, and a chemical tanker sailing in the North Atlantic with full-scale measurement is taken as the case study ship for validation of voyage optimization.

It can be seen that the different capabilities in performance predictions of ship models could lead to obvious changes in

voyage optimization results, both in terms of route and fuel consumption. Firstly, using the ML cost functions in general can provide more fuel savings than using the empirical cost functions. Meanwhile, the cost functions based on empirical models show more substantially varied results, while using ML ship models presents more stable fuel savings in diverse sailing condition cases. Also, for calm sea sailings, the difference between optimizing power and fuel costs can be minor. However, when it comes to harsher sea sailing that includes more environmental changes, the deviations can become more noticeable. In addition, when including the variation in actual engine efficiency SFOC, it also shows considerable changes in the optimization performance toward energy efficiency, especially when environmental changes become more dramatic, leading to more varying power changes.

It can be concluded that the voyage optimization system can be quite sensitive to the formulation of the energy cost function, as well as integrated ship performance models. An inefficient formulation of the ship model can lead to an inaccurate energy cost function, which further results in invalid voyage planning. Meanwhile, the proper choice of the energy cost in terms of power and fuel, as well as the hull-propulsion-engine coupling effect, e.g., the efficiencies of the engine and propeller, are also essential to be considered in voyage optimization to achieve more effective planning in real operational environments, especially for sailings in more dramatically changing sea environment.

ACKNOWLEDGMENTS

The authors would like to acknowledge the funding from the project AUTOBarge, European Union's EU Framework Program for Research and Innovation Horizon 2020 under Grant Agreement No. 955768; the Swedish Vinnova project 2021-02768; the Lighthouse sustainable shipping program.

REFERENCE

- [1] Abebe, M., Shin, Y., Noh, Y., Lee, S., and Lee, I., 2020, "Machine learning approaches for ship speed prediction towards energy efficient shipping," *Applied Sciences*, 10(7), p. 2325.
- [2] Akbar, A., Aasen, A. K., Msakni, M. K., Fagerholt, K., Lindstad, E., and Meisel, F., 2021, "An economic analysis of introducing autonomous ships in a short - sea liner shipping network," *International Transactions in Operational Research*, 28(4), pp. 1740-1764.
- [3] Chen, T., and Guestrin, C., "Xgboost: A scalable tree boosting system," *Proc. Proceedings of the 22nd acm sigkdd international conference on knowledge discovery and data mining*, pp. 785-794.
- [4] Dalheim, Ø. Ø., and Steen, S., 2020, "Added resistance and speed loss of a ship found using onboard monitoring data," *Journal of Ship Research*, 64(02), pp. 99-117.
- [5] Dijkstra, E., 1959, "A note on two problems in connexion with graphs," *Numerische Mathematik*, 1(1), pp. 269-271.
- [6] Faltinsen, O. M., "Prediction of resistance and propulsion of a ship in a seaway," *Proc. 13th Symposium on Naval Hydrodynamics*, Tokyo, pp. 505-529.
- [7] Guang, S., "Mathematical modeling of ship speed-loss due to wind and seas," *Proc. OCEANS'87*, IEEE, pp. 494-499.
- [8] Gupta, P., Rasheed, A., and Steen, S., 2022, "Ship performance monitoring using machine-learning," *Ocean Engineering*, 254, p. 111094.
- [9] Holtrop, J., and Mennen, G., 1982, "An approximate power prediction method," *International Shipbuilding Progress*, 29(335), pp. 166-170.
- [10] Kim, M., Hizir, O., Turan, O., Day, S., and Incecik, A., 2017, "Estimation of added resistance and ship speed loss in a seaway," *Ocean Engineering*, 141, pp. 465-476.
- [11] Lang, X., and Mao, W., 2020, "A semi-empirical model for ship speed loss prediction at head sea and its validation by full-scale measurements," *Ocean Engineering*, 209, p. 107494.
- [12] Lang, X., and Mao, W., 2021, "A practical speed loss prediction model at arbitrary wave heading for ship voyage optimization," *Journal of Marine Science and Application*, 20(3), pp. 410-425.
- [13] Lang, X., Wu, D., and Mao, W., "Benchmark Study of Supervised Machine Learning Methods for a Ship Speed-Power Prediction at Sea," *Proc. International Conference on Offshore Mechanics and Arctic Engineering*, American Society of Mechanical Engineers, p. V006T006A018.
- [14] Lee, S.-J., Sun, Q., and Meng, Q., 2023, "Vessel weather routing subject to sulfur emission regulation," *Transportation Research Part E: Logistics and Transportation Review*, 177, p. 103235.
- [15] Moreira, L., Vettor, R., and Guedes Soares, C., 2021, "Neural network approach for predicting ship speed and fuel consumption," *Journal of Marine Science and Engineering*, 9(2), p. 119.
- [16] Sang, Y., Ding, Y., Xu, J., and Sui, C., 2023, "Ship voyage optimization based on fuel consumption under various operational conditions," *Fuel*, 352, p. 129086.
- [17] Ships, I., 2015, "marine technology—Guidelines for the assessment of speed and power performance by analysis of speed trial data," ISO: Geneva, Switzerland.
- [18] Tarelko, W., and Rudzki, K., 2020, "Applying artificial neural networks for modelling ship speed and fuel consumption," *Neural Computing and Applications*, 32(23), pp. 17379-17395.
- [19] Townsin, R., and Kwon, Y., 1983, "Approximate formulae for the speed loss due to added resistance in wind and waves."
- [20] Vitali, N., Prpić-Oršić, J., and Soares, C. G., 2020, "Coupling voyage and weather data to estimate speed loss of container ships in realistic conditions," *Ocean Engineering*, 210, p. 106758.
- [21] Wang, H., Mao, W., and Eriksson, L., 2019, "A Three-Dimensional Dijkstra's algorithm for multi-objective ship voyage optimization," *Ocean Engineering*, 186, p. 106131.
- [22] Wen, S., Jin, X., Zheng, Y., and Wang, M., 2023, "Probabilistic coordination of optimal power management and voyage scheduling for all-electric ships," *IEEE Transactions on Transportation Electrification*.
- [23] Yu, H., Fang, Z., Fu, X., Liu, J., and Chen, J., 2021, "Literature review on emission control-based ship voyage

optimization," *Transportation Research Part D: Transport and Environment*, 93, p. 102768.

[24] Yuan, Z., Liu, J., Zhang, Q., Liu, Y., Yuan, Y., and Li, Z., 2021, "A practical estimation method of inland ship speed under

complex and changeful navigation environment," *IEEE Access*, 9, pp. 15643-15658.

[25] Zis, T. P., Psaraftis, H. N., and Ding, L., 2020, "Ship weather routing: A taxonomy and survey," *Ocean Engineering*, 213, p. 107697.